Development of Boundary Layer of Highly Elastic Flow of the Upper Convected Maxwell Fluid over a Stretching Sheet

M. Mohamadali
Department of Mechanical and Aerospace Engineering,
Science and Research Branch, Islamic Azad University, Tehran, Iran
E-mail: mmohamadali@gmail.com

N. Ashrafi*
Department of Mechanical and Aerospace Engineering,
Science and Research Branch, Islamic Azad University, Tehran, Iran
E-mail: n_ashrafi@hotmail.com
*Corresponding author

Received: 12 November 2015, Revised: 20 March 2016, Accepted: 24 April 2016

Abstract: High Weissenberg boundary layer flow of viscoelastic fluids on a stretching surface has been studied. The flow is considered to be steady and two dimensional. Flows of viscoelastic liquids at high Weissenberg number exhibit stress boundary layers near walls. These boundary layers are caused by the memory of the fluid. Upon proper scaling and by means of an exact similarity transformation, the non-linear momentum and constitutive equations of each layer transform into the respective system of highly nonlinear and coupled ordinary differential equations. Effects of variation in pressure gradient and Weissenberg number on velocity profile and stress components are investigated. It is observed that the value of stress components decrease by Weissenberg number. Moreover, the results show that increasing the pressure gradient results in thicker velocity boundary layer. It is observed that unlike the Newtonian flows, in order to maintain a potential flow, normal stresses must inevitably develop in far fields.

Keywords: Boundary Layer, High Weissenberg Flow, Nonlinear Viscoelastic Fluid, Similarity Solution

Reference: Mohamadali, M., Ashrafi, N., "Development of Boundary Layer of Highly Elastic Flow of the Upper Convected Maxwell fluid over a Stretching Sheet", Int J of Advanced Design and Manufacturing Technology, Vol. 9/ No. 2, 2016, pp. 35-44.

Biographical notes: M. Mohamadali received his PhD in Mechanical Engineering from the University of IAU, Science and Research Branch, in 2015. His current research interest includes boundary layer in Non-Newtonian fluids. **N. Ashrafi** is assistant professor of Mechanical engineering at the University of IAU, Science and Research Branch, Iran. He received his PhD in Mechanical engineering from the University of Western Ontario of Canada. His current research focuses on Non-Newtonian fluid dynamics and nonlinear mechanics.

1 INTRODUCTION

The flow of a liquid within a thin film over stretching plate is often encountered in most manufacturing processes. Examples include extrusion of plastic sheets, fabrication of adhesive tapes, and application of coating layers onto rigid substrates. Coating processes demand a smooth glossy surface to meet the requirements for best appearance and optimum service properties such as low friction, transparency and strength. Due to the moving surface, the main flow is closed to the extruded material while the far field stays almost stagnant. In view of such applications Crane [1] initiated the analytical study of boundary layer flow due to a stretching sheet. He assumed the velocity of the sheet to vary linearly as the distance from the slit and obtained an analytical solution. The work of Crane was subsequently extended mostly on both Newtonian and non-Newtonian (inelastic) boundary layer flows (See for example [2-5]) and only a few works on viscoelastic and elastic boundary layer flows [6]. Also the fluid employed in materials processing or protective coatings are in general viscoelastic, there have been little work done on the problem of flow of these fluids film on a stretching surface. In this connection, Hassanien [7] studied the second-grade fluid boundary layer over a linearly stretching sheet. The study was on boundary layer approximations of Newtonian flows [8] in order to simplify the governing equations. Here boundary layer equations were solved by a similarity method for elastic flows of Weissenberg numbers (*Wi*) of up to 0.2. The upper-convected Maxwell fluid is a class of visco-elastic fluid that can explain characteristics of the fluid relaxation time. It excludes complicated effects of shear-dependent viscosity and thus allows one to emphasize the influence of fluid's elasticity on characteristics of its boundary layer. So far, the exact solutions corresponding to the unsteady flow of a Maxwell fluid induced by the impulsive motion of a plate between two side walls perpendicular to the plate is developed employing the Fourier sine transforms [9]. Furthermore, Shateyi [10] studied the MHD flow of UCM past a vertical stretching sheet in a Darcian porous medium under the influence of thermophoresis, thermal radiation and a uniform chemical reaction for Weissenberg number as high as unity. Moreover the unsteady flow of Maxwell fluid induced over oscillating accelerated sheet was investigated in [11]. In another work, Hayat et al. used Homotopy method to simulate the flow and heat transfer of an UCM fluid over a moving permeable surface in a parallel free stream with the convective surface boundary condition [12]. Recently time-dependent three-dimensional boundary layer flow of a Maxwell fluid over a stretched sheet has been investigated by Homotopy method [13].

In the above viscoelastic flows the governing equations are scaled by Reynolds number only (similar to Newtonian fluids). Effect of viscoelasticity and normal stresses are therefore not properly presented. It is already reported that even at low Reynolds and high Weissenberg numbers, a boundary layer develops in the flow of viscoelastic fluid [14]. Additionally formation of normal stresses in viscoelastic flows is reported in many experiments which were done in high Weissenberg condition [23]. High Weissenberg flows mean long relaxation time in which the velocity of fluid vanishes at the wall and particles away from the wall travel long distances within one relaxation time so that particles close to the wall travel only a short distance. This leads to creating boundary layer in the shear stress [15]. The viscoelastic boundary layer is formed in a thin region closer to the wall in which the relaxation terms are recovered.

Up to now the boundary layer equations for the UCM fluids in two-dimensional flow along a flat boundary for high Weissenberg numbers are derived [15-16]. It was shown by that scaling parameters in view of the high Weissenberg condition and taking the leading terms of the upper convected Maxwell fluid governing equations result in the viscoelastic boundary layer development of order Wi^{-1}.Similar studies on the Phan-Thien-Tanner (PTT) and the Giesekus fluids results in the boundary layer development of order $Wi^{-1/3}$ and order $Wi^{-1/2}$ respectively [17]. This phenomenon can also be physically interpreted that "elastic" boundary layers for the Phan-Thien–Tanner and Giesekus fluid are similar to those for the upper-convected Maxwell model and arise when the dimensionless parameter measuring the size of the quadratic term is small. In fact, if the quadratic term is not small, the PTT model will have "viscometric" boundary layers in which it behaves like a generalized Newtonian fluid [18]. For the Giesekus model, the viscometric behaviour is different in that the shear stress remains bounded at infinite shear rate. Using an implicit function, the existence of solutions for viscoelastic boundary layer which arises from spatially periodic perturbations of uniform shear flow was addressed [19]. Also, the well-posedness of boundary layer equations for time-dependent flow of a UCM fluid in the limit of high Weissenberg and Reynolds numbers was analyzed [20]. Furthermore, a systematic perturbation procedure to solve the initial value problem for creeping flow of the UCM fluid at high Weissenberg number is formulated [21]. For instance, citing an analogy between a viscoelastic medium and an electrically conducting fluid containing a magnetic field, Ogilvie and Proctor [22] showed that the dynamics of the Oldroyd-B fluid in the limit of large Weissenberg number corresponds to that of a magnetohydrodynamic (MHD) fluid in the limit of large magnetic Reynolds number. In some

aspects, the problem of high Weissenberg number asymptotic for viscoelastic flows is similar to high Reynolds number asymptotic for Newtonian flows. The boundary layer also arises in high Weissenberg number flows since the convected derivative terms become essential at a short distance from the wall, leading to the formation of the aforementioned sharp boundary layer in the stresses [15].
The aim of this work is study of the boundary layer formation in high Weissenberg flow of UCM fluids past a stretching plate using similarity transformation. The stretching rate is assumed to be proportional to the ratio of horizontal distance on the direction. Using similarity transformation, the partial differential governing equations are transformed to a set of ordinary differential equations. The ordinary differential equations are then integrated numerically using a Runge–Kutta subroutine and shooting technique. Typical results for the velocity and stress profiles are presented.

2 GOVERNING EQUATIONS

The steady flow of a viscoelastic fluid over a (linearly) stretching sheet ($U_s = bx$) is brought to attention here. Consider two-dimensional steady flow of an Upper Convected Maxwell fluid occupying the half-plane $y > 0$. The fluid is flown by the movement of a thin elastic sheet emerging from a narrow slit at the origin of a Cartesian coordinate system under investigation shown schematically in Fig. 1. The continuity and momentum equations are written as [23]:

$$\nabla.\boldsymbol{V} = 0 \tag{1}$$

$$\rho(\boldsymbol{V}.\nabla)\boldsymbol{V} = \nabla\boldsymbol{T} - \nabla p \tag{2}$$

Where $\boldsymbol{T} = T_{ij}$ is the extra-stress tensor, $\boldsymbol{V} = (u, v)$ is the velocity field, p and ρ are the pressure and density respectively.
For a UCM fluid, the stress tensor, $\boldsymbol{T}$, can be related to the deformation-rate tensor as [23]:

$$\boldsymbol{T} + \lambda\overset{\nabla}{\boldsymbol{T}} = \eta(\nabla\boldsymbol{V} + (\nabla\boldsymbol{V})^t) \tag{3-1}$$

$$\overset{\nabla}{\boldsymbol{T}} = (\boldsymbol{V}.\nabla)\boldsymbol{T} - (\nabla\boldsymbol{V})\boldsymbol{T} - \boldsymbol{T}(\nabla\boldsymbol{V})^t \tag{3-2}$$

Where λ and η are the relaxation time and viscosity respectively and the symbol ∇ stands for the upper-convected derivative. Here, the Cartesian axes are assigned to the flow with the x-axis being along the plate and the y-axis normal to it (Fig. 1). The governing equations may be rewritten in dimensionless form by introducing typical scales for length, velocity, stress and pressure as follows [16]:

$$x' = x/L,\ \ y' = y/L,\ \boldsymbol{V}' = \boldsymbol{V}/U,\ \boldsymbol{T}' = \boldsymbol{T}/(\eta U/L),\ p' = p/(\eta U/L) \tag{4}$$

Where the capitals and primes represent reference and dimensionless values respectively. The reference velocity of stretching sheet is assumed to be $U=bL$. The dimensionless form of the governing equations is obtained by substituting the dimensionless parameter Eq. (4) into governing equations (1-3):

$$\nabla.\boldsymbol{V}' = 0 \tag{5-1}$$

$$\mathrm{Re}(\boldsymbol{V}'.\nabla)\boldsymbol{V}' = \nabla\boldsymbol{T}' - \nabla p' \tag{5-2}$$

$$\boldsymbol{T}'Wi^{-1} + ((\boldsymbol{V}'.\nabla)\boldsymbol{T}' - (\nabla\boldsymbol{V}')\boldsymbol{T}' - \boldsymbol{T}'(\nabla\boldsymbol{V}')^t) = Wi^{-1}(\nabla\boldsymbol{V}' + (\nabla\boldsymbol{V}')^t) \tag{5-3}$$

Where $Re=\rho UL/\eta$ is the Reynolds number, and $Wi=\lambda U/L$ is the Weissenberg number characterizing the elastic effects [1]. The no slip condition on the sheet and the far field condition boundary in dimensionless form are:

$$\bar{u}(\bar{x},0) = \bar{x}, \quad \bar{v}(\bar{x},0) = 0 \tag{6-1}$$

$$\bar{u}(\bar{x},\infty) = 0 \tag{6-2}$$

The basic reason for the formation of viscoelastic boundary layer is quite simple to elaborate. The convected derivatives in the constitutive relation vanish at the wall, forcing the stresses to be viscometric. However, at high Weissenberg number, the convected derivative terms become important at a short distance from the wall, leading to the formation of a boundary layer in the stresses. To maintain the balance between inertial force, viscous and elastic stresses to the leading order, a self-consistent set of scaling of variables is proposed [15]:

$$y' = \bar{y}/Wi,\ u' = u(\bar{x},\bar{y})/Wi,\ v' = \bar{v}(\bar{x},\bar{y})/Wi^2$$
$$T_{11}' = Wi\,\bar{T}_{11}(\bar{x},\bar{y}), T_{12}' = \bar{T}_{22}(\bar{x},\bar{y}), T_{22} = \bar{T}_{22}(\bar{x},\bar{y})/Wi \tag{7}$$

Substituting the above scalings into Eqs. (5) and keeping only the leading order terms in the rescaled equations, the scaled continuity and momentum equations in the boundary layer become as follows [21]:

$$\frac{\partial\bar{u}}{\partial\bar{x}} + \frac{\partial\bar{v}}{\partial\bar{y}} = 0 \tag{8-1}$$

$$\frac{\partial\bar{T}_{11}}{\partial\bar{x}} + \frac{\partial\bar{T}_{12}}{\partial\bar{y}} = \frac{\partial p}{\partial x} \tag{8-2}$$

$$0 = \frac{\partial p}{\partial y} \tag{8-3}$$

And the stresses equations in the boundary layer are obtained from Eq. (5-3):

$$\bar{T}_{11} + \bar{u}\frac{\partial \bar{T}_{11}}{\partial \bar{x}} + \bar{v}\frac{\partial \bar{T}_{11}}{\partial \bar{y}} - 2\frac{\partial \bar{u}}{\partial \bar{x}}\bar{T}_{11} - 2\frac{\partial \bar{u}}{\partial \bar{y}}\bar{T}_{12} = 0 \tag{9-1}$$

$$\bar{T}_{12} + \bar{u}\frac{\partial \bar{T}_{12}}{\partial \bar{x}} + \bar{v}\frac{\partial \bar{T}_{12}}{\partial \bar{y}} - \bar{T}_{22}\frac{\partial \bar{u}}{\partial \bar{y}} - \bar{T}_{11}\frac{\partial \bar{v}}{\partial \bar{x}} = \frac{\partial \bar{u}}{\partial \bar{y}} \tag{9-2}$$

$$\bar{T}_{22} + \bar{u}\frac{\partial \bar{T}_{22}}{\partial \bar{x}} + \bar{v}\frac{\partial \bar{T}_{22}}{\partial \bar{y}} - 2\bar{T}_{12}\frac{\partial \bar{v}}{\partial \bar{x}} - 2\bar{T}_{22}\frac{\partial \bar{v}}{\partial \bar{y}} = 2\frac{\partial \bar{v}}{\partial \bar{y}} \tag{9-3}$$

The scaled governing equations do not now contain Weissenberg number, so that the solutions of this system, i. e. the velocity and stress components are also independent of the Weissenberg number.

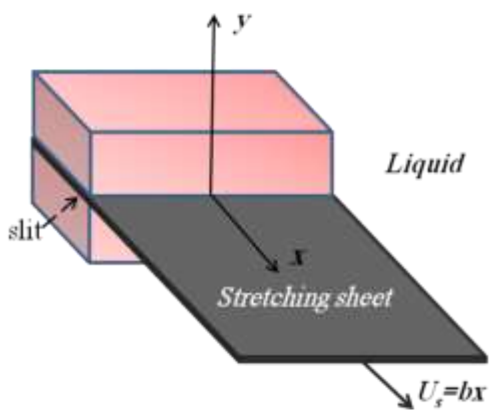

Fig. 1 Schematic diagram showing the physical configuration and coordinate system

The practical importance of this similarity with respect to Weissenebrg number consists of the fact that it suffices to find the solution to the boundary layer problem only once in terms of the above dimensionless variables.

3 SIMILARITY TRANSFORMATION

In order to solve the governing equation subject to the viscoelastic boundary layer, several similarity transformations were tried among which the following set appears to be computationally useful:

$$\xi(\bar{x},\bar{y}) = \frac{\bar{y}}{\bar{x}},\quad u(\bar{x},\bar{y}) = \bar{x}f\,'(\xi), T_{11}(\bar{x},\bar{y}) = \tau_{11}(\xi), T_{22}(\bar{x},\bar{y}) = \tau_{22}(\xi), T_{12}(\bar{x},\bar{y}) = \tau_{12}(\xi), \tag{10}$$

Where ξ is similarity variable and f, τ_{11}, τ_{12} and τ_{22} are unknown similarity functions and prime is derivation respect to the similarity variable ξ. Next using these transformations in Eq. (8-1), gives the normal velocity component by:

$$v(\bar{x},\bar{y}) = \bar{x}(2f(\xi) - \xi f\,'(\xi)) \tag{11}$$

In terms of the new variables, the transformed momentum and stress equations, i.e. Eqs. (8)- (9) can be rewritten as:

$$-\xi\tau_{11}'(\xi) + \tau_{12}'(\xi) = C \tag{12-1}$$

$$\tau_{11}(\xi) - 2\tau_{11}'(\xi)f(\xi) - 2\tau_{11}(\xi)(f\,'(\xi) - \xi f\,''(\xi)) - 2\tau_{12}(\xi)f\,''(\xi) = 0 \tag{12-2}$$

$$\tau_{12}(\xi) - 2f(\xi)\tau_{12}'(\xi) + \tau_{11}(\xi)(2f(\xi) + 2\xi f\,'(\xi) + \xi^2 f\,''(\xi)) - \tau_{22}(\xi)f\,''(\xi) = f\,''(\xi) \tag{12-3}$$

$$\tau_{22}(\xi) - 2\tau_{22}'(\xi)f(\xi) + \tau_{22}(\xi)(2f\,'(\xi) - \xi f\,''(\xi)) - 2\tau_{12}(\xi)(2f\,'(\xi) - \xi f\,''(\xi)) = -2(f\,'(\xi) + \xi f\,''(\xi)) \tag{12-4}$$

Where the integration constant C can be interpreted as a pressure gradient and the prime indicates derivation with respect to the similarity variable ξ. The boundary conditions are:

$$f(0) = 1,\quad f\,'(0) = 1,\quad f\,'(\infty) = 0 \tag{13}$$

The no-slip boundary conditions are imposed at the wall, however, due to the singularity of transformed equation on the wall at $\xi = 0$, it is not possible to integrate right from the wall [24, 25]. Expanding the velocity similarity function, f, at a minute distance above the plate (meaning ξ^*) returns the following approximation for $f(\xi)$ [24]:

$$f(\xi^*) = f\,''(0)\frac{\xi^{*2}}{2!} + O(\xi^{*3}) \tag{14}$$

In the same manner, the other similarity functions are expanded as follows [25]:

$$\begin{aligned} \tau_{11}(\xi^*) &= a_0 + a_1\xi^* + \ldots \\ \tau_{12}(\xi^*) &= b_0 + b_1\xi^* + \ldots \\ \tau_{22}(\xi^*) &= c_0 + c_1\xi^* + \ldots \end{aligned} \quad (15)$$

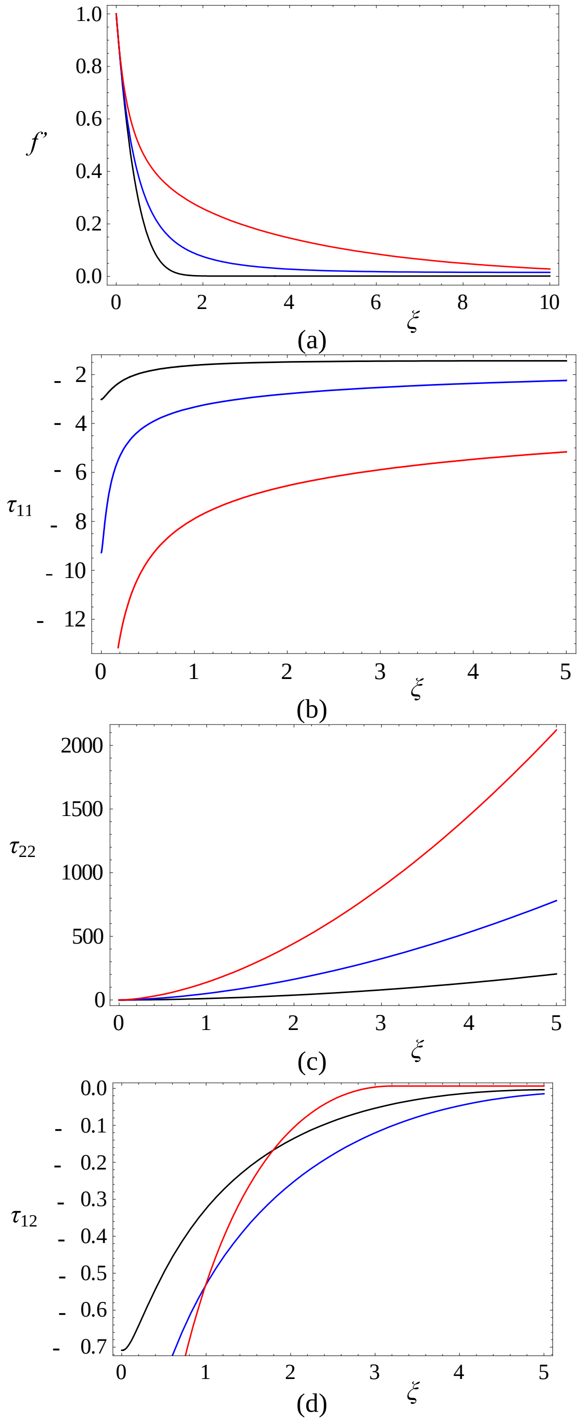

(—— C= 0 —— C = -0.5 —— C = -1.5)

Fig. 2 Velocity and stress profiles for several values of pressure gradient constant, C

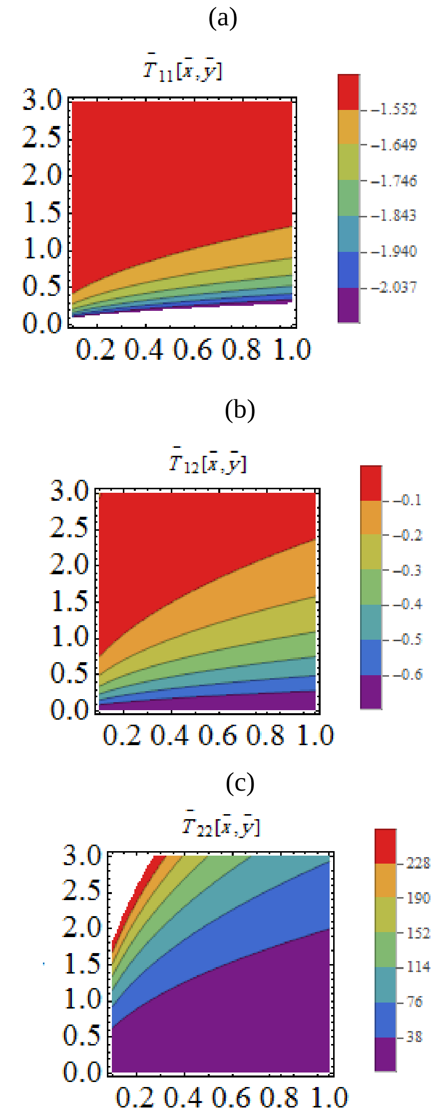

Fig.3 Scaled stress components in *x-y* plane in the absence of pressure gradient

Substituting the expanded functions in Eqs. (14) and (15) for a very close distance above the wall of nearly $\xi^* = 10^{-4}$ into the Eqs. (12), the constants are evaluated as:

$$a_0 = -\frac{2}{3} f''(0)^2, \quad b_0 = \frac{f''(0)}{3}, \quad c_0 = -\frac{2}{3} \qquad (16)$$

$$a_1 = 0, \; b_1 = -\frac{f'''(0)}{3}, \; c_1 = 0$$

It appears, in the above expressions, that the coefficients of the similarity functions contain independent parameters, $f''(0)$ and $f'''(0)$. In what follows, however, a relation between these two parameters can be established. The parameter $f''(0)$ is pertinent to the wall shear stress as it determines τ_{12} on the wall, while the parameter $f'''(0)$ may be given a physical interpretation by substituting the Eqs. (14) and (15) in transformed momentum equation (12-1) for $\xi \to 0$ in near wall region, which gives:

$$f'''(0) = -3C \tag{17}$$

(a)

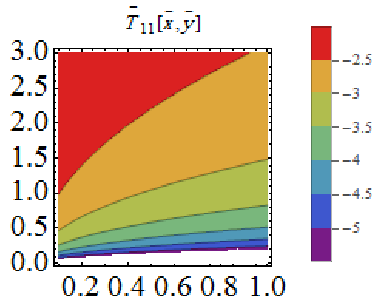

(b)

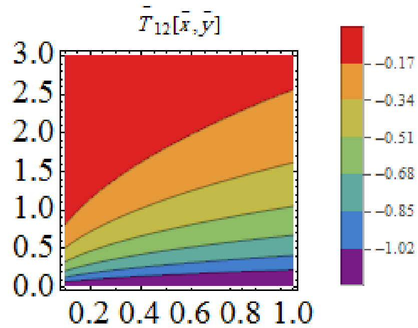

(c)

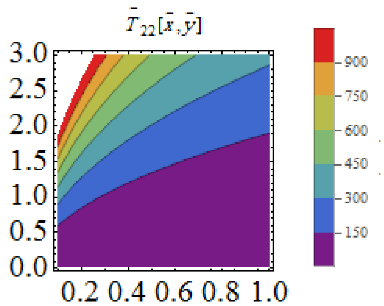

Fig.4 Scaled stress components in *x-y* plane for *C* = -0.5

4 NUMERICAL METHOD

The non-linear differential equations (8) together with the boundary conditions (13-16) constitute a boundary value problem (BVP) which is solved numerically by the shooting technique (see, for example [26]). In doing so, inevitably the following function changes are introduced. The resulted BVP is equivalent to a system of six first order differential equations [26]:

$$f'(\xi) = f_2(\xi) \tag{18-1}$$

$$f''(\xi) = f_2'(\xi) \tag{18-2}$$

$$-\xi\tau_{11}'(\xi) + \tau_{12}'(\xi) = C \tag{18-3}$$

$$\tau_{12}(\xi) - 2f(\xi)\tau_{12}'(\xi) + \tau_{11}(\xi)(2f(\xi) + 2\xi f_2(\xi) + \xi^2 f_2'(\xi)) - \tau_{22}(\xi) f_2'(\xi) = f_2'(\xi) \tag{18-4}$$

$$\tau_{11}(\xi) - 2\tau_{11}'(\xi) f(\xi) - 2\tau_{11}(\xi)(f_2(\xi) - \xi f_2'(\xi)) - 2\tau_{12}(\xi) f_2'(\xi) = 0 \tag{18-5}$$

(a)

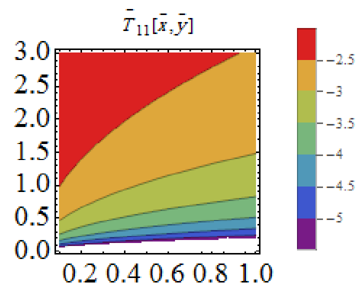

(b)

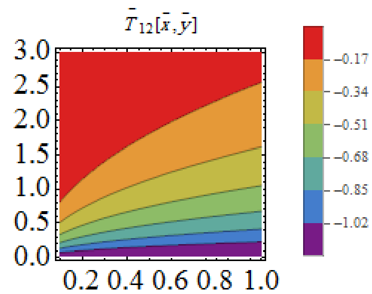

(c)

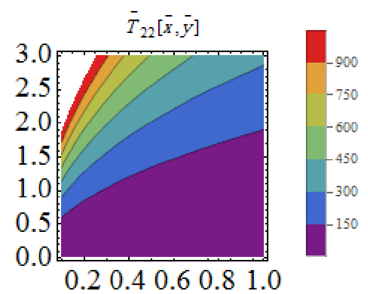

Fig.5 Scaled stress components in x-y plane for *C* = -1.5

$$\tau_{22}(\xi)-2\tau_{22}'(\xi)f(\xi)+\tau_{22}(\xi)(2f_2(\xi)-\xi f_2'(\xi))$$
$$-2\tau_{12}(\xi)(2f_2(\xi)-\xi f_2'(\xi))=-2(f_2(\xi)+\xi f_2'(\xi)) \quad (18\text{-}6)$$

To numerically solve the above equations, the infinite value of ξ must be replaced by a finite value of ξ (say $\xi\infty$) which is sufficiently large to satisfy the asymptotic condition. Here the value of 1000 turned out to be appropriate. Consequently equations (18) are integrated numerically by fourth order Runge–Kutta scheme from $\xi = \xi^*$ to $\xi = \xi_\infty$ with Eqs. (14)-(17) and guessed trail values $f''(0)$ which should satisfy the right-end boundary condition in Eq.(14). The Newton–Raphson scheme is employed to correct the arbitrary guess value such that the numerical solution will eventually satisfy the required boundary conditions to a precision of 10^{-4}. For further details on the numerical procedure, the reader is referred to [26]. As the first set of results, the values of $f''(0)$ for various pressure gradients are tabulated in Table. 1. This shows that $f'''(0)$ is related to the coefficient of the pressure gradient C and the wall shear stress [24].

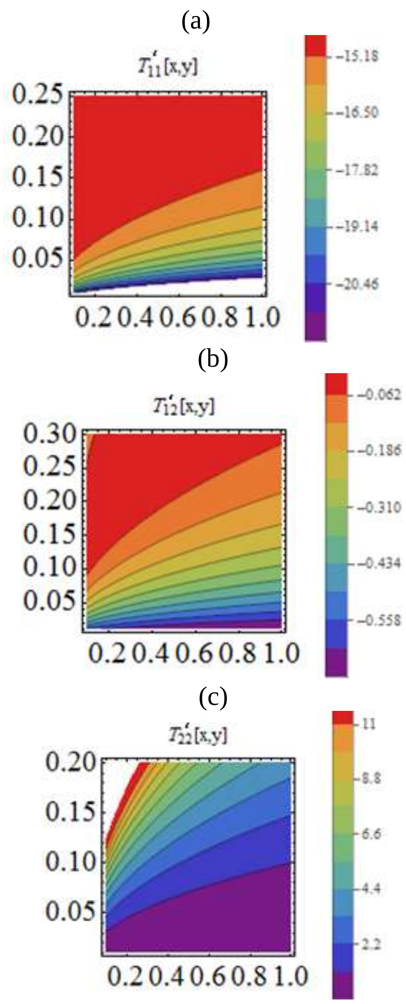

Fig. 6 Dimensionless stress components on a plate in the *x-y* plane for $C = 0$ for $Wi = 10$

5 RESULTS AND DISCUSSION

In this section the boundary layer formed by the flow of viscoelastic fluid over stretching sheet is presented. The flow is at high Weissenberg number and low Reynolds number. Within the boundary layer, therefore, the flow variables such as velocity, shear and normal stresses are evaluated for several values of pressure gradients.

Fig. 2a shows variation of velocity profiles $f'(\xi)$ with ξ for different pressure gradients, C. It can be seen that the velocity profiles decrease continuously to zero with the increase of the similarity parameter. Additionally, it is clear that increasing the values of C results in increasing the magnitude of velocity function causing velocity boundary layer to thicken.

Figure 2b reveals that regardless of the pressure gradient, the normal stress function in the flow direction, τ_{11}, monotonically reaches a constant value. In other fashion, the normal stress component perpendicular to the flow, τ_{22},

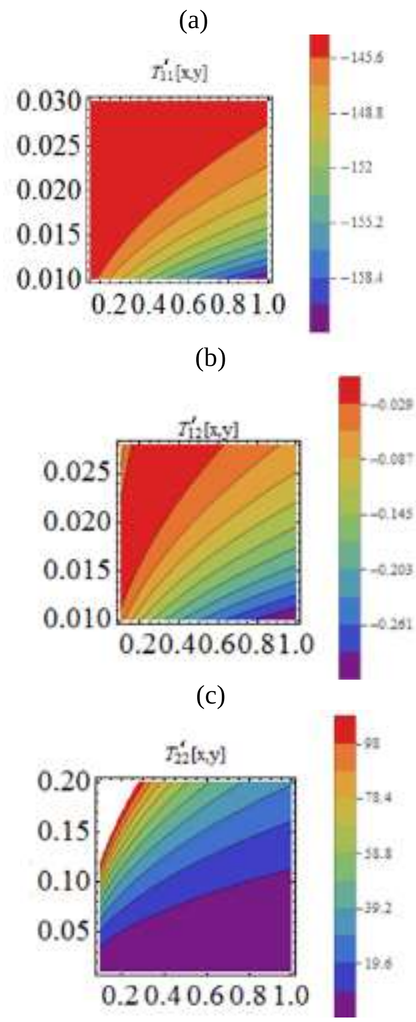

Fig. 7 Dimensionless stress components on a plate in the *x-y* plane for $C = 0$ for $Wi = 100$

Grows by increasing ξ as shown in Fig. 2c. Additionally, the values of both normal stress functions increase with increase of pressure gradient. Also, the value of shear stress, τ_{12}, decreases monotonically to zero, implying that the stresses are non-existent shear force far from the plate. Finally, it is observed that the wall shear stress increases in line with increase of pressure gradient.

(a)

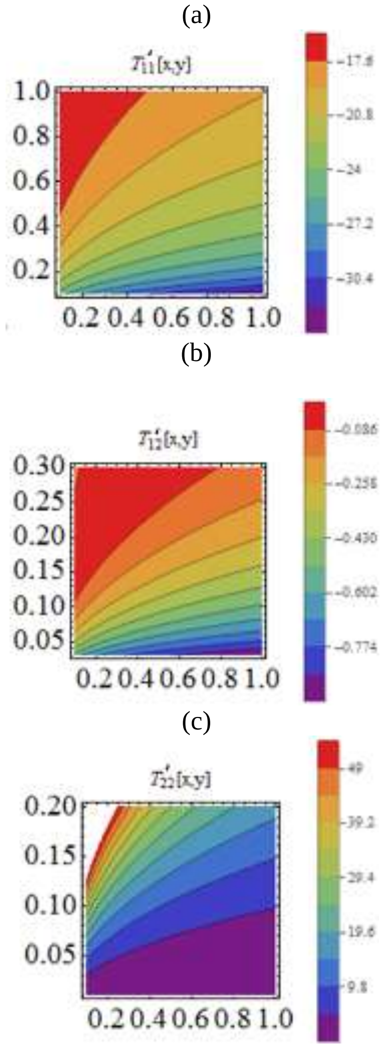

Fig. 8 Dimensionless stress components on a plate in the *x-y* plane for C = -0.5 for Wi = 10

In continuation, Figs. 3-5 show scaled stress components, near the stretching wall in x–y plane. The figures are arranged in a way that the pressure is increased incrementally in each row. Generally, the stress contours of first normal stress, and shear stress, are denser near the wall. On the contrary, an opposite behaviour is observed for second normal stress. This phenomenon is maybe explained that, in high Weissenberg flows, far from the solid boundary, the elastic property of the flow is dominant which leads to formation of normal stress in the absence of velocity gradient and elimination of the shear stress.

In this region the normal stress in the flow direction goes to a constant value and the other normal stress component, increases by distancing far from the plate. A point to make here is that, adjacent to the wall as the pressures gradient increases, the values of all stress components rise.

In continuation, Figs. 6-9 show dimensionless stress components, T'_{ij}, near the solid wall in x–y plane for Wi = 10 and 100 and pressure gradients equal to 0 and -1.5, respectively. Generally, the stress contours are denser near the wall. The viscoelastic boundary layer becomes thinner with increase of Wi number.

(a)

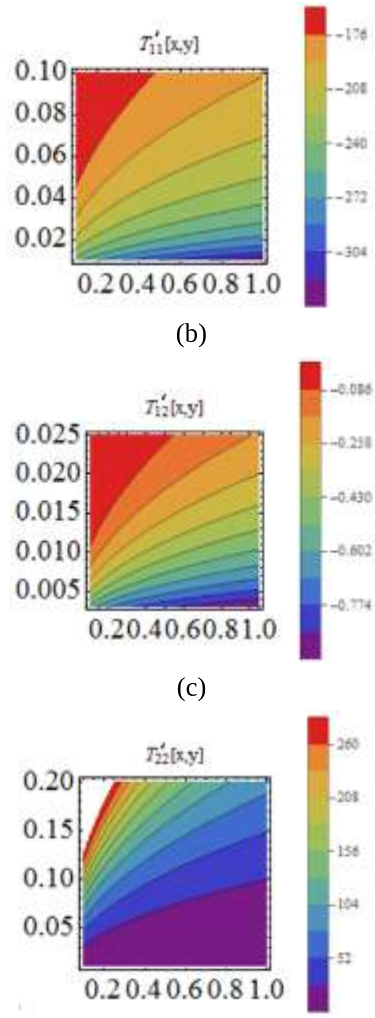

Fig. 9 Dimensionless stress components on a plate in the *x-y* plane for C = -0.5 for Wi = 100

Furthermore, to provide a better physical sense of the overall problem, the dimensionless streamlines and velocity vector are drawn in Figs. 10 for Wi equal to 10 in the absence of pressure gradient. As seen in this figure, far from the plate, the velocity is essentially vertical. This maybe pertinent to the normal stresses developed within the viscoelastic due to high elastic nature of high Weissenberg flow.

Table 1 Values of *f'*'(0) for various pressure gradients

C	*f'*'(0)
0	-2.0215
-0.5	-2.110
-1	-2.140
-1.5	-2.156
-2	-2.162

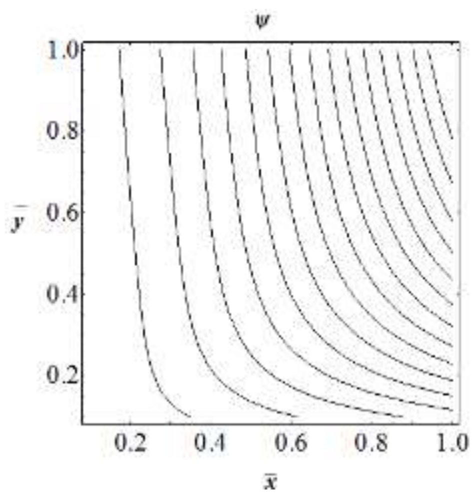

(a)

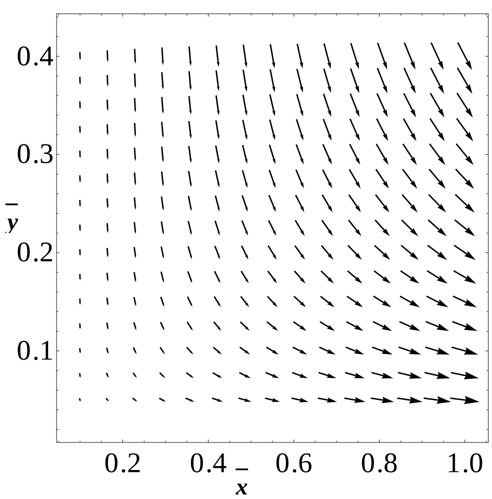

(b)

Fig. 10 Development of scaled (a) Stream lines and (b) Velocity vector field for viscoealstic boundary layer (C=0)

6 CONCLUSION

Stress boundary layer of highly elastic flow of the Upper Convected Maxwell fluid over a linear stretching sheet is studied numerically. Using similarity transformations, the scaled dimensionless momentum and constitutive equations are converted to a system of ordinary differential equations for which a numerical solution is sought. A custom-made shooting technique is devised to ensure arriving at credible solution of the derived highly coupled and highly nonlinear equations.

It can be concluded that, in general, the velocity boundary layer thickness increases with pressure gradient. As well, the values of both normal stress functions increase with increase of pressure gradient.

However, the normal stress function in the flow direction, τ_{11}, monotonically reaches a constant value. In other fashion, the normal stress component perpendicular to the flow, τ_{22}, grows by increasing the parameter ξ. Also, the value of shear stress, τ_{12}, decreases monotonically to zero, implying that the shear stress is non-existent force far from the plate.

Additionally, in high Weissenberg flows, far from the solid boundary, the elastic property of the flow is dominant. This fact, results in formation of normal stress in the absence of velocity gradient and elimination of the shear stress so that a "potential" flow is observed while, contrary to the Newtonian flow, the fluid velocity is essentially vertical to the plate. In this region the normal stress in the flow direction T_{11}, goes to a constant value and the other normal stress component, increases by distancing from the plate. Finally, it is observed that the value of stress components decrease by Weissenberg number.

REFERENCES

[1] Crane, L. J., "Flow past a stretching sheet", ZAMP, Vol. 21, 1970, pp. 645–647.

[2] Prasad, K. V., Santhi, S. R., and Datti, P. S:, "Non-Newtonian power-law fluid flow and heat transfer over a non-linearly stretching surface", Appl. Math., Vol. 3, No. 5, 2012, pp. 425-435.

[3] Xu, H., and Liao, S. J:, "Laminar flow and heat transfer in the boundary-layer of non-Newtonian fluids over a stretching flat sheet", Comput. Math. Appl., Vol. 57, 2009, pp. 1425-1431.

[4] Abel, M. S., Datti, P. S., and Mahesha, N., "Flow and heat transfer in a power-law fluid over a stretching sheet with variable thermal conductivity and nonuniform heat source", Int. J. Heat Mass Transfer, Vol. 52, 2009, pp. 2902–2913.

[5] Wang, C., "Analytic solutions for a liquid film on an unsteady stretching surface", Heat Mass Transfer, Vol. 42, 2006, pp.759–766.

[6] Ashrafi, N., Mohamadali, M., "High Weissenberg Number Stress Boundary Layer for the Upper

Convected Maxwell Fluid”, Proceedings of the ASME International Mechanical Engineering Congress & Exposition, Vol. 8B, Heat Transfer and Thermal Engineering, Montreal , 2014, pp. 201-207.

[7] Hassanien, I. A., “Flow and heat transfer on a continuous flat surface in a parallel free stream of viscoelastic second-order fluid”, Appl. Sci. Res., Vol. 49, 1992, pp. 335-344.

[8] Schichting., H., “Boundary Layer Theory”, sixth ed., McGraw Hill, New York, 1964, Chap 7.

[9] Hayat, T., Fetecau, C., Abbas, Z., and Ali, N., “Flow of a viscoelastic fluid with fractional Maxwell model between two side walls due to suddenly moved plate”, Nonlinear Anal. Real World Appl., Vol. 9, 2008, pp. 2288-2295.

[10] Shateyi, S., “A new numerical approach to MHD flow of a Maxwell fluid past a vertical stretching sheet in the presence of thermophoresis and chemical reaction”, Bound. Val. Prob., Vol. 196, 2013.

[11] Fetecau, C., Jamil, M., Fetecau, C., and Siddique, I., “A note on the second problem of Stokes for Maxwell fluids”, Int. J. Non-Linear Mech., Vol. 44, 2009, pp. 1085-1090.

[12] Hayat, T., Shehzad, S. A., and Alsaedi, A., “Study on three-dimensional flow of Maxwell fluid over a stretching surface with convective boundary conditions”, Int. J. Phys. Sci., Vol. 7, No. 5, 2012, pp.761-768.

[13] Awais, M., Hayat, T., Alsaedi, A., and Asghar, S., “Time-dependent three-dimensional boundary layer flow of a Maxwell fluid”, Computers & Fluids, Vol. 91, 2014, pp. 21–27.

[14] Rajagopal, K. R., Boundary layers in non-linear fluids, in: M.D.P. Monteivo Marques, Trends in Applications of Mathematics to Mechanics, in: Pittman Monographs and Surveys in Pure and Applied Mathematics, Vol. 77, Longman, New York, 1995.

[15] Renardy, M., and Wang, X., “Boundary layers for the upper convected Maxwell fluid”, J. Non-Newtonian Fluid Mech., Vol. 189, 2013, pp. 14–18.

[16] Renardy, M., “High Weissenberg number boundary layers for the upper convected Maxwell fluid”, J. Non-Newtonian Fluid Mech., Vol. 68, 1997, pp. 125-132.

[17] Hagen, T., and Renardy, M., “Boundary layer analysis of the Phan–Tien–Tanner and Giesekus model in high Weissenberg number flow”, J. Non-Newtonian Fluid Mech., Vol. 73, 1997, pp. 181–189.

[18] Renardy, M., “Prandtl boundary layers for the Phan-Thien Tanner and Giesekus fluid”, Z. Angew. Math. Phys., Vol. 66, 2014, pp. 1061- 1070.

[19] Renardy, M., “Wall Boundary Layers for Maxwell Liquids”, Arch. Rational Mech. Anal., Vol. 152, 2000, pp. 93–102.

[20] Renardy, M. and Wang, X., “Well-posedness of boundary layer equations for time-Dependent flow of Non-Newtonian fluids”, J. Math. Fluid Mech., Vol. 16, 2014, pp. 179–191

[21] Renardy, M., “The initial value problem for creeping flow of the upper convected Maxwell fluid at high Weissenberg number”, Math. Meth. Appl. Sci., Vol. 38, 2014, pp. 959–965.

[22] Ogilvie, G. I., Proctor, M. R. E., “On the relation between viscoelastic and magneto-hydrodynamic flows and their instabilities”, J. Fluid Mech., Vol. 476, 2003, pp. 389-409.

[23] Bird, R. B., Armstrong, R. C., “Dynamics of polymeric Liquids”, second ed., John Wiley & Sons, New York, 1987, Chap 5.

[24] [24] Evans, J. D., “Re-entrant corner flows of the Upper Convected Maxwell fluid,” Proc. Roy. Soc. A, Vol.461, 2005, pp.117–142.

[25] Renardy, M.,“A matched solution for corner flow of the upper convected Maxwell fluid”, J. Non-Newtonian Fluid Mech.,Vol. 58, 1995, pp. 83-89.

[26] Press, W. H., Teukolsky, S. A., Vetterling, W. T., and Flannery, B. P., Numerical Recipes (in Fortran 77), 2nd ed., Cambridge University Press, New York, 2007.Chap12.